

ORIGINAL ARTICLE

Characterization and climate response patterns of a high-elevation, multi-species tree-ring network in the European Alps

David Frank*, Jan Esper

Swiss Federal Research Institute WSL, Birmensdorf, Switzerland

Received 7 April 2004; accepted 15 December 2004

Abstract

We combine 53 ring width and 31 maximum latewood density data sets from a network of high-elevation tree sites distributed across the European Alps (43–48°N and 6–14°E). This network is analyzed to understand the climate, and in particular, the temperature signal, in terms of geography, species and measured parameter. These analyses will be useful for any subsequent climatic reconstruction. The first Principal Component (PC) of the ring width chronologies explains 20% of the network's variance and correlates significantly with the June–August summer season temperatures, while that of the density chronologies explains 69% of the variance and correlates with the wider April–September season. Of the four species considered, ring width records from *Picea abies*, *Larix decidua*, and *Pinus cembra* tend to show most similar responses to climate, with the *Abies alba* having a more unique response. The climatic signal of the density chronologies is rather independent of species and site ecology. It is quite strong across the network, although possibly weighted towards the higher-frequency domains. In comparison, the ring width chronologies display much greater site- and species-specific components in their climate response, with only elevation found to serve as an indicator for the level of seasonal temperature response. Climatic gradients across the network are shown to exist through spatial correlation and rotated Principal Component Analysis (PCA). These gradients are rather small, but show similar patterns to those observed in PCA of instrumental data. High correlations between temperature and *Latix decidua* are found despite concern over the presence of effects from the larch budmoth on the climatic signal. Similarly, the ring width parameter of *Pinus cembra* showed strong ability to serve as a proxy, notable in the context of this species to have poorer responses to temperature when considering maximum latewood density. The potential for a regional climatic reconstruction, using the networks PCs as predictors exists, as demonstrated by the high and consistent loadings across the network on the first PCs for both the ring width and density chronologies.

© 2005 Elsevier GmbH. All rights reserved.

Keywords: Dendroclimatology; Temperature; Ring width; Maximum latewood density; Network; Alps

Introduction

Tree-ring data currently play a prominent role in the characterization and assessment of climate variations prior to the instrumental period. The spatial scale of

tree-ring reconstructions ranges from local (e.g., Pederson et al., 2001; Schweingruber et al., 1988), to regional (e.g., Cook et al., 2003; Wilson and Luckman, 2003) to hemispheric (e.g., Briffa, 2000; Esper et al., 2002a; Jacoby and D'Arrigo, 1989). In detail, the potential for trees to serve as a proxy can depend on a variety of factors including species, altitude, site ecology, tree age, measured parameter, and

*Corresponding author. Tel.: +41 1 739 2282.

E-mail address: frank@wsl.ch (D. Frank).

standardization method, for example (Fritts, 1976; Schweingruber, 1996). It is widely known that ring width and maximum density variations from trees growing in high-latitude or -altitude treeline environments are sensitive to temperatures and can be used for their reconstruction (e.g., Jacoby and D'Arrigo, 1989; Esper, 2000; Briffa et al., 2002a; Esper et al., 2002a,b, 2003).

A multitude of tree-ring-based climate studies are reported from the Alps. These include local to sub-regional temperature reconstructions (e.g., Serre-Bachet et al., 1991; Nicolussi and Schiessling, 2001; Wilson and Topham, 2004; Büntgen et al., accepted), the assessment of isotopic signals in trees (Treydte et al., 2001), analyses of climatic conditions that resulted in extreme growth reactions in trees (e.g., Kienast et al., 1987; Neuwirth et al., 2004), and the effects of tree's stand status on the climate response (e.g., Meyer and Bräker, 2001), for example. More ecologically oriented studies from the Alps have considered the effect of disturbance regimes (e.g., Cherubini et al., 1996), and the climatic triggering of interannual density fluctuations along ecological gradients (e.g., Rigling et al., 2002). In addition to hundreds of ring width records, including many to study geomorphic processes (e.g., Baumann and Kaiser, 1999; Gärtner et al., 2003), more than 50 maximum latewood density chronologies from several coniferous species have been developed. Many of these chronologies were analyzed as a component of much larger European and Northern Hemisphere networks (Schweingruber and Briffa, 1996). Due to their high signal strength (Schweingruber et al., 1979; Briffa et al., 2002a) attention has been given to the maximum latewood density chronologies to reconstruct hemispheric temperature patterns (e.g., Briffa et al., 1998, 2002b).

Network analyses specifically focusing on the Alps include regional studies of smaller networks of ring width chronologies from the French Alps (Petitcolas and Rolland, 1996; Rolland et al., 2000), the Dolomites (Hüsken and Schirmer, 1993), and the Eastern (Urbinati et al., 1997) and Western (Motta and Nola, 1996) Italian Alps. Many of the studies from around the Alpine region that evaluate the climate sensitivity of trees do so along altitudinal gradients (e.g., Kienast et al., 1987; Dittmar and Elling, 1999; Rolland et al., 2000). Larger scale comparisons of, and reconstructions from, suitable high-elevation, potentially temperature sensitive ring width and density data are, however, broadly missing.

In this paper, we show such a network of high-elevation trees from the Western and Central European Alps, and analyze variations in terms of species, parameter (ring width vs. maximum latewood density), and geographical position, and focus on the characteristics and climate response patterns of the tree-ring

network. The analyses and results presented in this paper will set the foundations for two alpine temperature reconstructions, based on both ring width and maximum latewood density data, in a following paper (Frank and Esper, accepted).

After this introduction, the basic tree-ring and instrumental data are presented in the section "Data". The section, "Chronological signals" considers only the chronologies and their various signals, through correlation and Principal Component Analysis (PCA). In the section, "Climate signals" we characterize the chronologies responses to climate, including spatial patterns of climate correlations, spatial autocorrelation and elevational differences. The last section contains a discussion of the main findings, and we convey our views on the potential of temperature reconstructions using this network and in this region.

Data

Tree-rings and detrending

Tree-ring sites were selected within the Central and Western Alp region from 43–48°N and 6–14°E, and, to maximize potential temperature sensitivity, above elevations of 1500 m a.s.l. *Picea abies* (L.) H. Karst., *Abies alba* Mill., *Larix decidua* Mill., and *Pinus cembra* L. are the four species considered (herein abbreviated as PCAB, ABAL, LADE and PICE). These species are widely distributed throughout the Alps and as such are already represented in dendrochronological data sets. Additional selection criteria were based on the time span of the chronology, sample size, species representation and tradeoffs therein. Ring width data exist for all sites and, if available, maximum latewood density was also included into the network data set. Data from W. Elling, H. Fritts, W. Hüsken, F. Meyer, B. Neuwirth, R. Niederer, C. Rolland, F. Schweingruber, F. Serre, L. Tessier and K. Treydte were incorporated into the network and are gratefully acknowledged.

The majority of the network sites (31) were developed by Schweingruber and collaborators, as part of a comprehensive ring width and density network of sites from around the Northern Hemisphere (Schweingruber et al., 1979, 1987; Briffa et al., 1988, 1998; Schweingruber and Briffa, 1996). Ten sites used in this network were developed by C. Rolland and collaborators. These sites have been included in analyses of the regional extent of pointer years (Rolland et al., 2000), long-term growth changes (Rolland et al., 1998) and teleconnections on a regional scale (Rolland, 2002). Other sites, incorporated in this network have been used in a wide variety of studies (e.g., LaMarche and Fritts, 1971; Tessier, 1981; Serre-Bachet et al., 1991; Hüsken and Schirmer, 1993; Dittmar and Elling, 1999, Meyer and

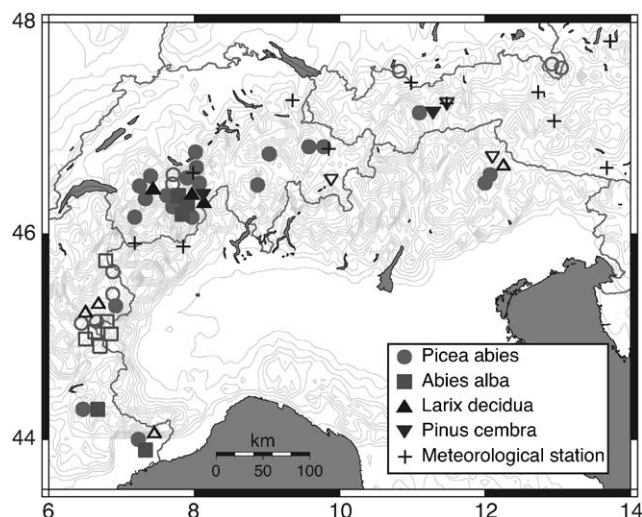


Fig 1. Map showing the locations of the 53 tree-ring sites included in the network. Sites are differentiated by species and whether ring width and maximum latewood density parameters were both available for a site (filled symbol) or only ring width (empty symbol). The locations of the 11 meteorological stations used to make the high-elevation gridded data (Böhm et al., 2001) are also shown. All tree-ring sites and meteorological stations are above 1500 m a.s.l.

Bräker, 2001; Treydte et al., 2001; Neuwirth et al., 2004).

All chronologies were screened with the program COFECHA (Holmes, 1983). In a few cases series were deleted based on this check. In total, chronologies from 53 sites are considered, 31 of which had density data (Fig. 1, Table 1). PCAB is the most dominant species represented in the network with 30 ring width chronologies. Sites are distributed across the Alpine arc with locally dense pockets in southwestern Switzerland and the central portion of the French Alps. Sites from both the Italian and Austrian Alps are broadly under represented within this network, in comparison to the high spatial density of chronologies within the Swiss and French Alps. ABAL sites are located towards the western and southern portions of the network, with the other three species more evenly distributed.

To remove the age trend and standardize the ring width data (Fritts, 1976), an adaptive power transform was first applied to all measurements to stabilize their variance (Cook and Peters, 1997), and then residuals from a spline with a 300-year frequency–response cutoff were taken (Cook and Peters, 1981). Such splines reduce the amplitude of waveforms with a period of 300 years by 50%. Density series were detrended by taking residuals from linear fits of any slope. These detrending methods should be sufficient to remove age-related growth trends, without removing significant climatic information on annual to multi-decadal timescales. Chronologies were averaged on a site-by-site basis using

a robust mean (Cook, 1985). They were adjusted for changing replication by utilizing the sample size information and the average correlation between series (Osborn et al., 1997), and truncated at a minimum sample size of five series. Maximum chronology spans and their lengths after truncation are listed in Table 1. After truncation the longest chronology in the network is a LADE site from southeastern France (1186–1974), and the shortest a LADE site from southwestern Switzerland (1899–1973). Median chronology lengths are 193 and 171 years for ring width and density after truncation, respectively. Forty-five of the 53 ring width and 26 of the 31 density chronologies cover the 1850–1973 period. Extension of this period, either towards more recent or towards earlier times, decreases the number of chronologies available for analysis. For example, for ring width and density, 16 (3) and 6 (1) chronologies span 1750–1973 (1750–1995), respectively.

Meteorological data

Temperature and precipitation data were kindly provided by R. Böhm. Instrumental data were subjected to homogeneity tests and adjustments, spatial and temporal analysis and then gridded on a 1×1 degree network (Auer et al., 2000; Böhm et al., 2001). In addition to individual station data, two temperature data sets are available: a low-elevation grid that covers a wide area with 106 gridpoints and a 16-point high-elevation grid, restricted to a band coinciding with the core of the Alpine chain. The high-elevation grid is based on data from 11 meteorological stations above 1500 m a.s.l. (Böhm et al., 2001), matching the elevation criteria for the tree-ring data. Station locations follow the alpine arc, but are more densely concentrated in the eastern portion of the network than the tree-ring data (Fig. 1). The common period for all of the high-elevation gridpoints is 1864–1998, with all 11 stations having the 1933–1998 common period. Both the high-elevation station and gridded data are used for the following analyses.

Chronology signals

Within site characteristics

As a basic assessment of chronology characteristics and signals, the average correlation coefficient between the individual series after detrending (R_{bar}) was computed for each chronology (Wigley et al., 1984). Average R_{bar} results are lower for ring width than for density, with LADE having the highest and PICE the lowest R_{bar} for both of these parameters (Fig. 2). We hypothesize LADE tends to have higher R_{bar} values

Table 1. Site locations used in this study

Site name	Species	Max. span	Crnl. Len.	Lat. (N)	Long. (E)	Elev. (m)	Contributor
Nizza, Foret d'Aillon	ABAL	1838–1975	116	43.88	7.33	1700	F. Schweingruber
Névache Sapin Moyen N.	ABAL	1803–1993	132	45.02	6.63	1600	C. Rolland
Tatz Stockwald	ABAL	1825–1980	132	46.33	7.78	1850	F. Schweingruber
Mittleri Hellelawald	ABAL	1812–1980	153	46.30	7.83	1510	F. Schweingruber
Col d'Allos	ABAL	1771–1975	153	44.27	6.57	1900	F. Schweingruber
Bardonecchia Sapin Supérieur N.	ABAL	1809–1993	154	45.03	6.68	1900	C. Rolland
Bürchen Bielwald	ABAL	1708–1980	190	46.28	7.83	1740	F. Schweingruber
Bardonecchia Sapin Moyen N.	ABAL	1767–1993	204	45.03	6.68	1700	C. Rolland
Tarentaise Sapin Moyen S.	ABAL	1741–1993	214	45.60	6.88	1600	C. Rolland
Montgenèvre Sapin Supérieur N.	ABAL	1745–1994	240	44.92	6.70	1780	C. Rolland
Névache Sapin Supérieur N.	ABAL	1727–1993	257	45.02	6.63	1850	C. Rolland
Riederalp VS Binna	LADE	1877–1973	75	46.37	8.03	1800	F. Schweingruber
Riederalp VS Aletschwald	LADE	1792–1974	126	46.40	8.02	2000	F. Schweingruber
Simmental, Iffigenalp	LADE	1681–1986	216	46.40	7.43	1900	F. Schweingruber
Fodara Vedla Alm	LADE	1520–1990	432	46.63	12.10	1970	W. Huesken
L'Orgere High	LADE	1524–1973	435	45.22	6.68	2100	L. Tessier
L'Orgere Low	LADE	1353–1958	577	45.22	6.68	1900	L. Tessier
Les Merveilles	LADE	988–1974	789	44.05	7.45	2300	F. Serre-Bachet
Mt.Cenis	PCAB	1834–1975	116	45.27	6.92	1950	F. Schweingruber
Cortina d'Ampezzo (Nord)	PCAB	1737–1975	120	46.53	12.07	1820	F. Schweingruber
Riederalp VS Aletschwald	PCAB	1778–1974	129	46.40	8.02	2000	F. Schweingruber
Nizza, Foret d'Aillon	PCAB	1795–1975	134	43.88	7.33	1700	F. Schweingruber
Cold'Allos	PCAB	1792–1975	141	44.27	6.57	1900	F. Schweingruber
Tatz Stockwald	PCAB	1769–1980	149	46.33	7.78	1850	F. Schweingruber
Arosa GR Rot Tritt (Nord)	PCAB	1690–1975	159	46.80	9.68	1940	F. Schweingruber
Mittleri Hellelawald	PCAB	1793–1980	171	46.30	7.83	1510	F. Schweingruber
Pierre Avoi VS	PCAB	1772–1979	172	46.12	7.18	1900	F. Schweingruber
Névache Epicéa Moyen N.	PCAB	1774–1993	180	45.02	6.63	1600	C. Rolland
Arosa GR Arlenwald (Slid)	PCAB	1785–1975	180	46.80	9.68	2000	F. Schweingruber
Lötschental Shady	PCAB	1660–1995	184	46.39	7.78	1970	B. Neuwirth and K. Treydte
Tarentaise Epicéa Supérieur N.	PCAB	1778–1993	192	45.60	6.88	1900	C. Rolland
Stubaital, Milderaun Ahn	PCAB	1745–1975	192	47.13	11.28	1850	F. Schweingruber
Grindelwald Nord (N3)	PCAB	1786–1995	193	46.60	8.03	1700	F. Schweingruber
Maurienne Epicéa Supérieur N.	PCAB	1790–1993	195	45.28	6.88	1950	C. Rolland
Ochsenkopf	PCAB	1674–1991	200	47.53	10.82	1530	W. Elling
Lötschental oWG-SCH, CH	PCAB	1768–1998	200	46.43	7.82	1900	F. Schweingruber
Simmental, Iffigenalp	PCAB	1532–1986	202	46.40	7.43	1900	F. Schweingruber
Grindelwald Süd (S3)	PCAB	1774–1995	211	46.65	8.02	1960	F. Schweingruber
Suaiza, TI	PCAB	1695–1988	240	46.43	8.87	1520	F. Schweingruber
Lauenen BE Briichli	PCAB	1701–1976	243	46.42	7.32	1500	F. Schweingruber
Névache Epicéa Supérieur N.	PCAB	1738–1993	250	45.02	6.63	1850	C. Rolland
Cortina d'Ampezzo (Slid)	PCAB	1660–1975	251	46.53	12.07	1900	F. Schweingruber
Simmental, St. Stephan, Gyrs	PCAB	1690–1986	259	46.52	7.40	1900	F. Schweingruber
Lötschental Sunny	PCAB	1660–1998	264	46.43	7.81	1980	B. Neuwirth and K. Treydte
Bürchen Bielwald	PCAB	1707–1980	268	46.28	7.83	1740	F. Schweingruber
Rothspiel	PCAB	1680–1990	274	47.56	13.02	1615	W. Elling
Wasserbett, Watzmannscharte	PCAB	1651–1990	302	47.57	12.95	1525	W. Elling
Obersaxen, Meierhof, GR	PCAB	1537–1995	373	46.73	9.03	1580	F. Schweingruber
Riederalp VS Aletschwald	PICE	1788–1974	105	46.40	8.02	2000	F. Schweingruber
Patscherkofel	PICE	1752–1967	129	47.22	11.47	2200	H. Fritts
Stubaital, Milderaun Ahn	PICE	1822–1975	134	47.13	11.28	1850	F. Schweingruber
Muottas de Schlarigna	PICE	1662–2001	320	46.48	9.88	2200	J. Esper and P. Bebi
Fodara Vedla Alm	PICE	1474–1990	476	46.63	12.10	1970	W. Huesken

because of both its high sensitivity to climatic (temperature) conditions in the year of ring formation, and the frequent common pointer years caused by periodic attacks of the larch budmoth (*Zeiraphera diniana* Guénée) (Weber, 1997).

When correlating the ring width and density chronologies from the same site with each other over the 1880–1974 period, the average (Pearson) correlation is 0.11 with a standard deviation of 0.12. The maximum correlation (0.34) was for a LADE site, and the minimum (−0.18) for an ABAL site. These rather low within-site correlations between ring width and density chronologies suggest that these two parameters contain largely different signals within the network. The two parameters are therefore treated separately in the following analyses.

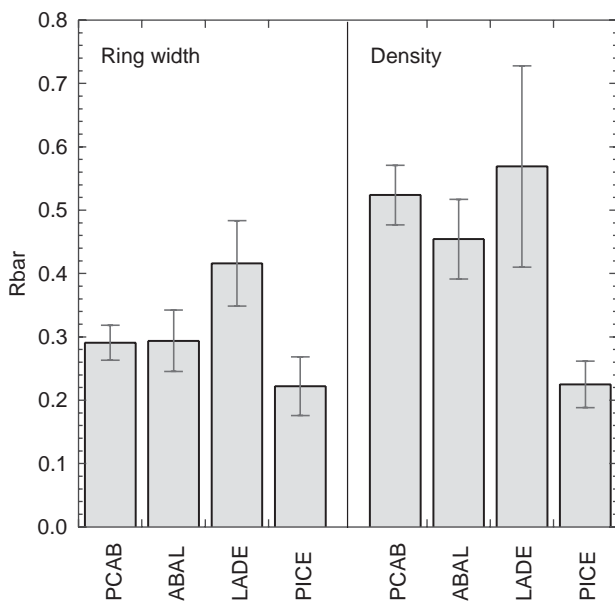


Fig. 2. Plots of the average interseries correlation (R_{bar}) of the tree-ring series after detrending for both ring width and density. Correlations were computed over the maximum length for every chronology. Error bars denote the ± 2 standard error range.

Species-to-species correlations

Pearson's correlations between all chronology pairs for the ring width and density parameters were computed, over the 1880–1974 period, to quantify the similarities in signal as a function of species. Results were grouped into correlations within and between all possible species combinations, and are summarized as the average correlation (and number of correlation pairs) for ring width and density (Table 2). Maximum latewood density correlations are much higher and less variable than their ring width counterparts, reflecting the largely species-independent signal strength of this parameter. PCAB and LADE tend to have the highest correlations for density comparisons. PICE tends to have the highest inter-correlations for ring width, but the lowest for density. Ring width correlations for the ABAL, followed by LADE are lower, with the only negative correlation of −0.07 occurring between these two species. The grand average correlation of all chronology pairs, independent of species, is 0.18 and 0.66 for ring width and density, respectively.

Spatial autocorrelation over the network

The above correlations do not consider the relative location of the tree sites. Therefore to assess the spatial autocorrelation over the network, average (Pearson) correlations as a function of distance (correlograms) are computed for all tree-to-tree pairs from the network (Fig. 3). Ring width and density data were correlated separately over the 1880–1974 period, and subsequently subdivided into comparisons made within the same species, and comparisons between different species. This time interval was chosen as it is covered by the majority of chronologies and still contains fairly well-replicated early instrumental temperature data.

The density series have much higher inter-correlations than their ring width counterparts, with maximum values of 0.81 and 0.70 within and between species,

Table 2. Mean correlations between (A) ring-width sites and (B) density sites as a function of species

	PCAB	ABAL	LADE	PICE
A				
PCAB	0.26 (435)	0.10 (330)	0.14 (210)	0.21 (160)
ABAL	—	0.33 (55)	−0.07 (77)	0.16 (55)
LADE	—	—	0.38 (21)	0.13 (35)
PICE	—	—	—	0.43 (10)
B				
PCAB	0.71 (210)	0.64 (105)	0.64 (63)	0.57 (42)
ABAL	—	0.62 (10)	0.62 (15)	0.52 (10)
LADE	—	—	0.73 (3)	0.60 (6)
PICE	—	—	—	0.52 (1)

Numbers in parenthesis are the number of correlation pairs.

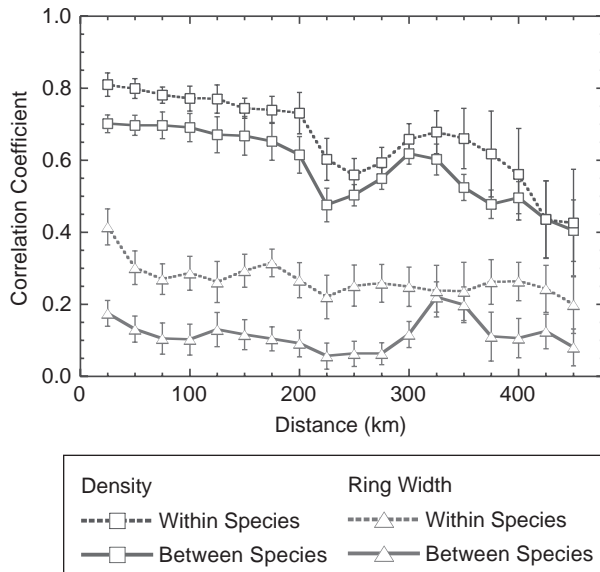


Fig. 3. Average correlations as a function of distance (correlograms) for tree-ring series, shown for correlations made within the same species (dashed) and correlations between different species (solid), for the ring width (triangles) and density (squares) parameters. Correlations were averaged in 50 km distance classes lagged 25 km, with the ± 2 standard error range shown.

respectively. These values decrease to around 0.4 in the 450 km distance class. Values for within species ring width data range from 0.42 to 0.20, occurring at the smallest and largest distance classes, respectively. A sharp decline is seen after the first distance class and then values fluctuate around a slight negative trend. In general, within species inter-correlations are higher than comparisons made between different species. Correlations between species tend to have values about 0.2 and 0.1 below those for the within species, for ring width and density, respectively, further indicating a more species-independent response of the density parameter to common climate.

Curious features in both the ring width and density data are significant departures from idealized smooth trends, such as those centered around 250 km in the density data, and the increase in values around 325 km in the between species ring width data. However, these features can be explained, as they are a by-product of the uneven distribution of the network chronologies. The ‘anomalously’ low correlations at around 250 km occur when the results are heavily influenced by the chronologies from the southwestern portion of the network (see Fig. 1). Lower correlations between this cluster and the dense cluster of chronologies in southwestern Switzerland devalue the result at this distance class. The southwestern chronologies are under more of a Mediterranean influence than the majority of the network, and these results further point to the climatic texture of the network. The ‘anomalous’ increases in the between species correlations, in contrast, seem to result

from correlations between the PICE and LADE rich eastern part of the network in combination with the dense cluster of chronologies from southwestern Switzerland (see Fig. 1).

PC analysis

To further elucidate patterns inherent in the tree-ring network, PCA was performed using the 45 ring width and 26 density chronologies that share the 1850–1973 common period. For density, the first four Principal Components (PCs), containing 82% of the variance in the density network, were retained and subjected to varimax rotation (Richman, 1986). While the first few unrotated PCs will contain information that is more or less common between the series, the varimax rotation redefines the PC axes and maximizes the spread of the individual loadings. This tends to result in spatially more interpretable loadings (Richman, 1986).

From the maps of the loadings on the first three rotated axes, spatial clustering and gradients are evident (Fig. 4a–c). The first rotated factor explains 37% of the variance and has highest loadings from the dense concentration of chronologies in southwestern Switzerland, with diminishing loadings east and south. Loadings on the second factor (24% variance) are highest towards the east, with declining values towards the west and south. The third rotated factor explains 14% of the variance and is largely the opposite of the second factor, with highest loadings in southeastern France and diminishing towards the north and east.

For ring width, the first seven PC components explain 66% of the variance. Site loadings on the first rotated factor (13% variance) are similar to the patterns observed for the density loadings (Fig. 4d). Highest loadings occur in the central portion of the network, with a tendency for higher values persisting eastward and lower values southward. Loadings on the second rotated factor (10% variance) have a reversed pattern with highest loadings in the southwestern portion of the network and lowest loadings towards the northeast. The patterns seen with the ring width chronologies are somewhat noisier than for the density chronologies, which we again attribute to more site-specific variance in the ring width network. The same analysis for ring width but using only PCAB resulted in very similar patterns, suggesting that species differences and, for example, the concentration of ABAL in the southwestern portion of the network do not heavily bias these results.

The PC patterns seem to be largely independent of species and in general help define gradients of chronology response and clustering over the network. The major east–west gradients that are seen are likely analogous, and governed by the same factors as the primarily east–west contours of the first two PCs of

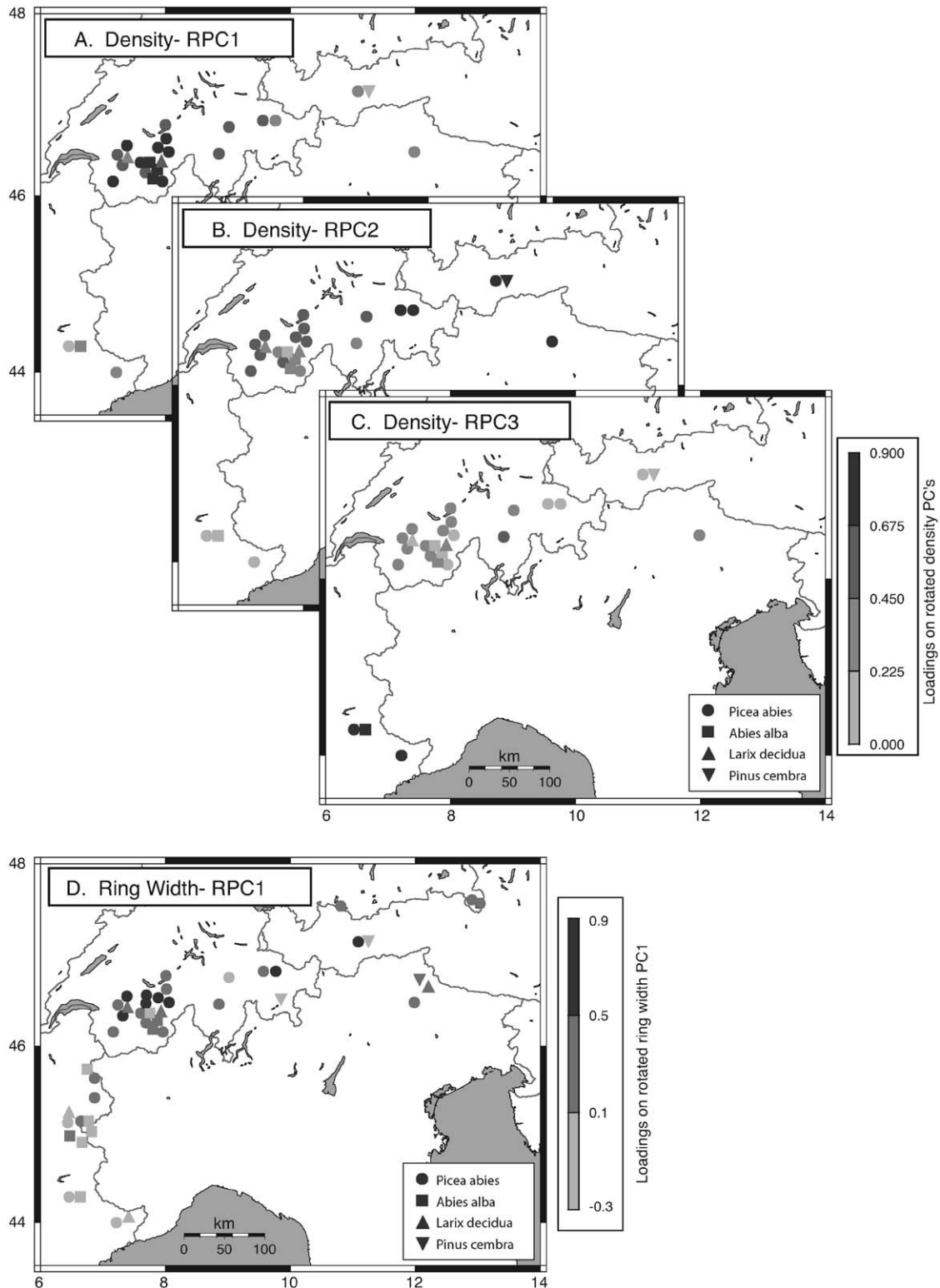


Fig. 4. Map of loadings of site chronologies on varimax-rotated principal components, (A–C) for the first three of four retained density chronology factors and (D) the first of seven rotated ring width chronology factors. All calculations are based on the 1850–1973 common period. Chronologies not meeting these length requirements did not enter the calculations.

meteorological station data performed by Böhm et al. (2001). This major east–west gradient appeared even though the Böhm et al. (2001) analysis included a much

wider North–South range of stations than the tree-ring network data, as the instrumental data were not confined to the alpine chain.

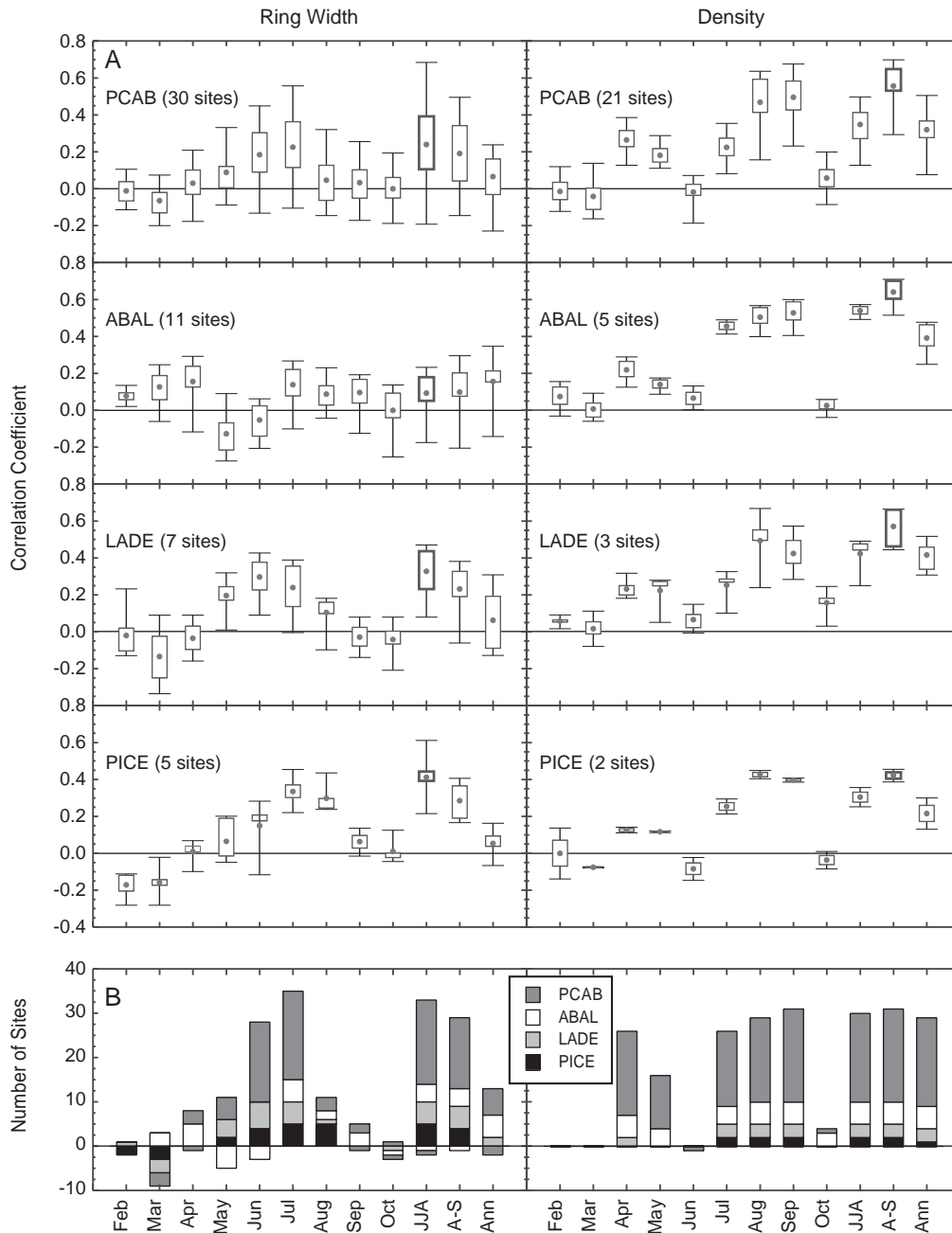


Fig. 5. Plot of correlations between monthly and seasonal climate data and ring width and density chronologies. All correlations were computed over 1880–1974 between chronologies and the nearest high-elevation grid point. (A) Box plots showing the range of values for each species and each meteorological season. The horizontal bars denote the minimum and maximum values, the 25–75% quantile range is contained within the box, and the mean correlation denoted by the dot. (B) Histogram of the number of sites with a significant ($p < 0.1$) correlation with monthly or seasonal data. The JJA season best integrates ring width chronologies and the A–S season the density chronologies.

Climate signals

Correlation with climate

To assess the climate response of the tree-ring sites, correlations between all chronologies and monthly and seasonal meteorological data from the nearest high-elevation gridpoint were computed. All correla-

tions were calculated over the 1880–1974 period, common to all but four chronologies. Results for monthly temperature correlations of February–October of the current growing season, of the June–August (JJA), April–September (A–S), and annual means are shown in Fig. 5. Analyzed but not shown are results for precipitation and the year prior to the current growing season.

Correlations with precipitation result in few network wide patterns for ring width and density chronologies. Numerous sites have negative correlations with summer precipitation, which we largely attribute to the inverse covariation of summer temperature and precipitation in the Alps, but perhaps also indicative of some moisture limitations. Six of the 11 ABAL ring width chronologies show positive correlations ($p < 0.1$) with May precipitation of the current growing season. Negative correlations with February precipitation are seen at a number of the density sites, perhaps related to delay in the onset of the growing season due to late winter snow.

There are very few significant correlations for temperature and density in the prior season, with the notable exception of 17 of 31 sites having a significant positive ($p < 0.1$) response to the previous March. Currently, we have no explanation for this. Ring width response to the prior season is more variable. Generally, the LADE and PICE chronologies have a tendency for a positive response to much of the previous year. The PCAB and ABAL chronologies have negative correlations with previous summer temperatures and positive correlations during the surrounding spring and autumns. Eight of the 11 ABAL chronologies have positive correlations ($p < 0.1$) to prior November temperatures. This same feature was noted by Rolland (1993), where it was speculated that warmer November temperatures characterize a mild winter, which is important as this species seems to be sensitive to winter frost (Rolland, 1993).

The density response of all species to current season temperatures is rather consistent (Fig. 5, right). There is a positive response to April and May and then again to July, with peak values for all species in August and September. Correlations for the JJA, A–S, and annual periods are positive, with the A–S season having the highest correlations. Correlations for this A–S season are at very similar levels to those of average August–September.

The PCAB, LADE and PICE ring width chronologies show positive responses to growing season temperatures, generally with: PCAB chronologies responding to June and July, LADE to May–July, and PICE to June–August temperatures (Fig. 5, left). ABAL series differ with their tendency towards positive correlations with March and April, negative correlations with May and June, and then again positive correlations with late summer temperatures. These results combined with the positive response to May precipitation mentioned above, suggest the greater drought sensitivity of this species within the network during early summer. ABAL displays a higher positive correlation to annual than to summer temperatures.

Those months or seasons for each site with significant positive or negative correlations at the $p < 0.1$ level were tallied and are summarized in Fig. 5b. For ring width,

peak significant correlations occur in June and July. Of the seasonal correlations shown, JJA displays the highest common response to temperatures: $\frac{19}{30}$ PCAB, $\frac{4}{11}$ ABAL, $\frac{5}{7}$ LADE, and $\frac{5}{5}$ PICE ring width chronologies have significant positive correlations for this season. In comparison, all 31 density chronologies have significant positive correlations during the A–S season. Based on these results, the JJA and A–S seasons are used for further ring width and density comparisons, respectively. Correlation results for ring width and the June–July season are very similar to those for JJA for most of the chronologies, but JJA seems to provide a more uniform warm season basis that considers all species (i.e., ABAL and PICE). While these seasons are certainly not optimized for every chronology and perhaps not for every species, they provide a reasonable basis for comparison. Other studies of Northern Hemisphere conifer networks have concluded similarly (e.g., Briffa et al., 2002a) and used these same seasons for ring width and density parameters from higher-latitude trees.

The grand average correlation, over the 1880–1974 period, of all ring width chronologies to JJA temperatures is 0.24, while the density series have an average correlation of 0.56 with the A–S season. These numbers integrate all sites regardless of the individual response structure. The correlations for the individual months also follow this tendency of the density series to have substantially higher correlations than the ring width.

The common signals within this network can be tested through ordinary PCA. Using the 1850–1973 period covered by 45 ring width and 26 density chronologies, the first PC explain 20% and 69% of the variance, respectively. For ring width, all chronologies, except for a single ABAL site, load positively on this component, showing that PC 1 represents common information that spans the entire network. When this first eigenvector is correlated with monthly or seasonal temperature from a single gridpoint near the center of the network, peak values for July are obtained. This signal diminishes in the earlier and later months, but remains positive between April and September. For density, all chronologies have positive loadings on PC 1, with values between 0.13 and 0.23. This eigenvector, when correlated with monthly temperature data, shows peak correlations to August and September, and positive values in April, May and July. Patterns of the monthly correlations of the first PCs are similar to the tallied results in Fig. 5b. The relatively high explained variance (particularly for density chronologies) with only a few PCs is indicative of high common signals and demonstrates that PCA can capture common climatic information from across the network.

To further explore the climate response of the ring width and density parameters, tree-ring chronologies and the seasonal (JJA and A–S) instrumental temperature data were filtered with a 10-year spline. Both the

Table 3. High- and low-frequency correlation comparison

Species	Ring width (Lf>Hf)	Density (Lf>Hf)
PCAB	7/30	2/21
ABAL	8/11	0/5
LADE	5/7	1/3
PICE	4/5	0/2

Lf = low-pass filtered, and Hf = high-pass filtered data.

high- and low-pass fractions were retained, effectively splitting the data into high- and low-frequency components. These high- and low-pass fractions have average correlations of 0.12 for both ring width and density series, indicating their near independence. Correlations between the high-passed tree-ring and high-passed instrumental data, and the low-passed tree-ring and low-passed instrumental data were computed and compared with the unfiltered correlations. Tree-ring series were then classified into two groups based on whether the high- or low-pass fractions had higher or lower correlations with their, respectively, filtered met data (Table 3). This comparison suggests that the density chronologies transport a greater fraction of their climate related variance in the higher frequency domains, whereas the ring width series (particularly for ABAL, LADE and PICE) contain a greater fraction of their signal, although on a lower level, in the lower-frequency domains.

Spatial correlation patterns

Maps of the correlation coefficients between ring width and JJA, and density and A–S temperatures show spatially highly variable patterns for ring width and less variability for density (Fig. 6, note the different scales of correlations). Site specific ecology can play a strong role in the ring width response, as seems to be the case here. The density chronologies from the very southwestern portion of the network have lower correlations with A–S temperatures, likely resulting from their proximal location to the Mediterranean Sea. Their greater distance to the center of the instrumental network could also be partly responsible.

To further quantify the climatic gradients over the network, distance-grouped average correlations (correlograms) for instrumental-to-instrumental and tree-to-instrumental pairs were calculated (Fig. 7). For the instrumental-to-instrumental correlations, the results for the two seasons JJA and A–S are very similar. In both, a slight decrease in mean correlation with increasing distances occurs, but still remains above 0.80 at 450 km. The stable and high correlations even at such distances point to the relatively homogeneous nature of

the high-elevation seasonal temperature data across the network.

For the tree-to-instrumental correlations, density and ring width correlations are 0.66 and 0.22 at the nearest distance class, respectively. Values for both the ring width and density generally decrease, reaching values of 0.49 and 0.09 after 550 km, however, results for the ring width data tend to be more ‘noisy’. To determine if there was a bias due to geographic position (e.g., the southwestern sites tend to be further from the instrumental stations), the same analysis with correlation anomalies (with respect to each chronologies average correlation with the 11 stations) was performed. This result also showed similar decreasing trends, although slightly noisier for the ring width comparisons. Despite the rather small differences in the climate data over the network, decreasing values are still observed with increasing distances showing that the trees are still sensitive to even the slight differences in the regional instrumental records.

For comparative purposes, the tree-to-tree and tree-to-instrumental relationships are re-plotted (Fig. 7b). We find it interesting that the correlation levels for the tree-to-tree comparisons are similar to those for the tree-to-climate comparisons, and they arguably decrease in a somewhat similar fashion with increasing distances. This strengthens the picture of the common forcing for the chronologies and suggests that the average commonalities within the ring width and density chronologies are quite similar to those that are captured by the seasonal instrumental data. Further, the decreasing correlations of the tree-to-tree comparisons with increasing distance are likely related to the climatic gradient over the Alpine region, as evidenced by the arguably similar decreasing trends in the tree-to-instrumental comparisons.

Vertical correlation patterns

In an attempt to explain the climate response as a function of site locations and the available metadata, comparison with elevation data proved to be relevant. The correlation results from above are plotted as a function of elevation above sea level (Fig. 8, note the different scales for elevation). Accordingly, the ring width chronologies tend to show higher correlations with increasing elevation. The results shown are dominated by the PCAB. Linear fits to the few ABAL and PICE sites show similarly increasing trends, while a fit to the LADE has a negative slope. However, this regression is heavily weighted by a LADE chronology from 2300 m a.s.l. from the southwestern portion of the network. The linear that fits to the density chronologies do not yield any significant correlations, although over a smaller range of elevations. While the natural upper timberline in the Alps varies by over 300 m (e.g.,

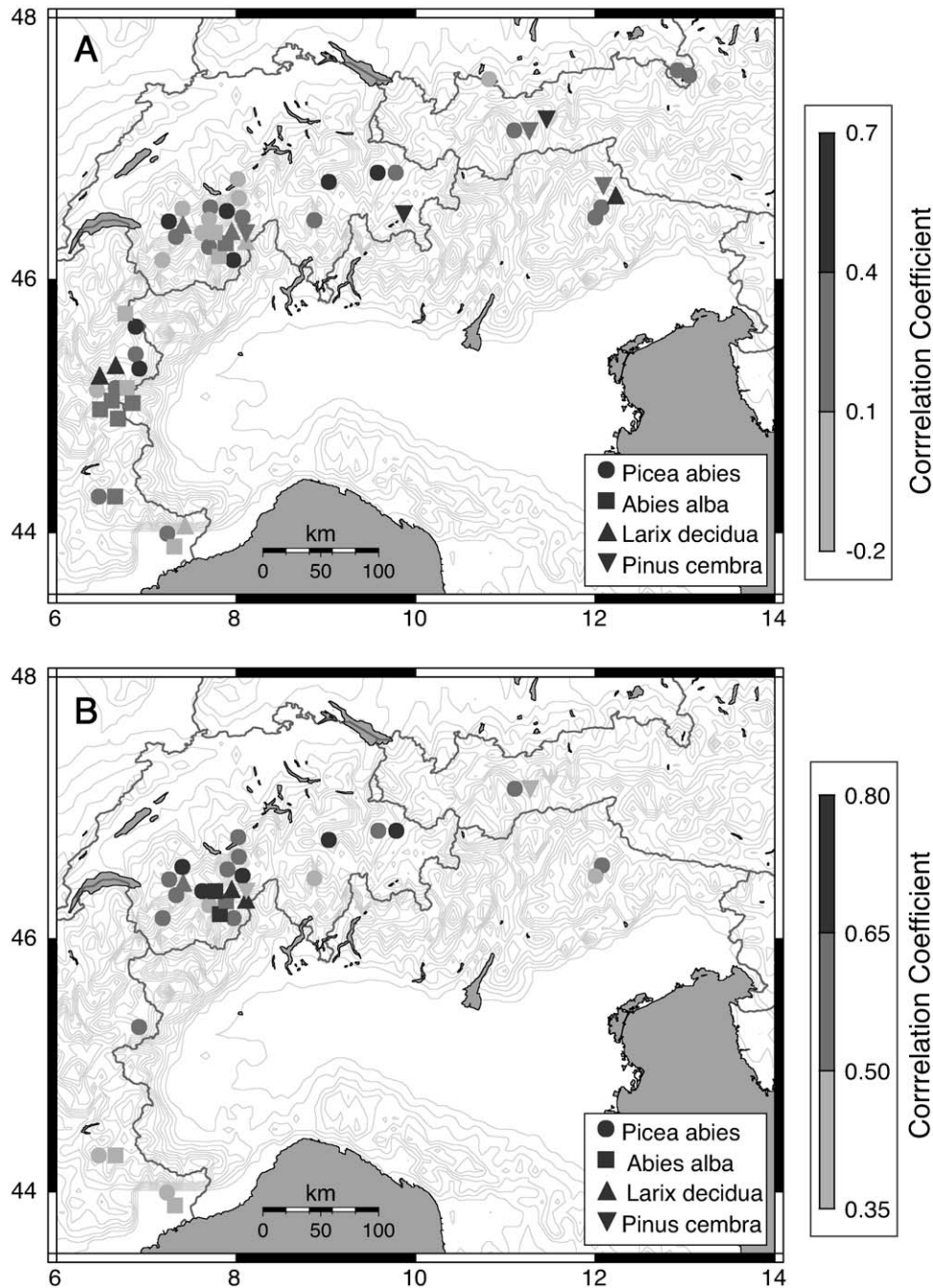


Fig. 6. Map of site correlations with seasonal climate grouped into three correlation classes, shown (A) for ring width and JJA temperature and (B) for density and A–S temperatures. Correlations were computed over the 1880–1974 period between tree sites and the nearest high-elevation grid point (see Fig. 1). Note the different scales. Ring width chronologies display a higher variability related to site-specific factors.

Brockmann-Jerosch, 1919; Paulsen et al., 2000), the site elevation data still seems to indicate that better temperature signals for dendroclimatological studies are obtained towards the upper treeline for the ring width data. Within the smaller elevational range of high-elevation density sites, this relationship does not appear.

Discussion

The analysis of the Central and Western alpine network and the climate response of the ring width and density records within this network will serve as a basis to develop regression-based models to reconstruct summer temperature variability over the past centuries

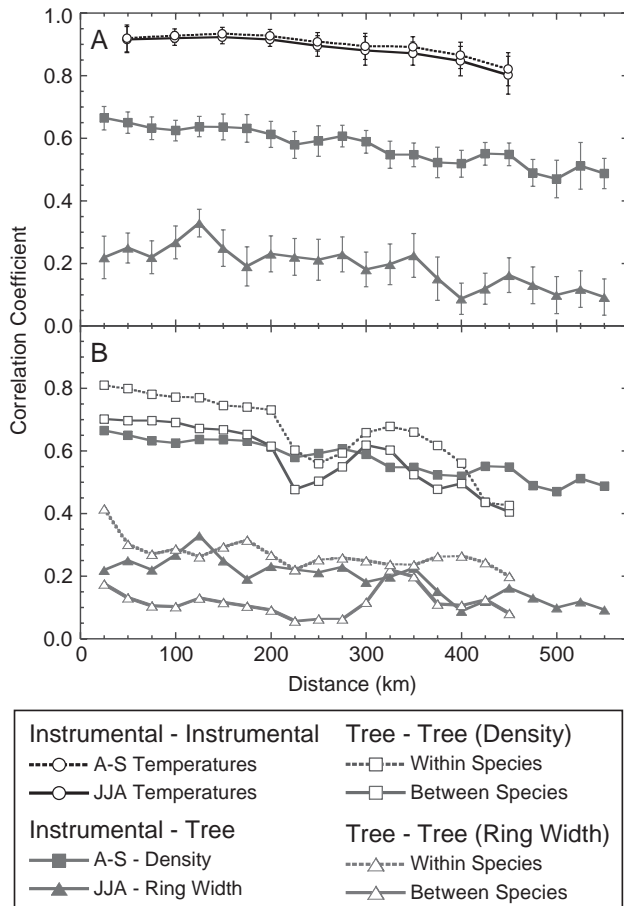


Fig. 7. Average correlations as a function of distance (correlograms) for instrumental-to-instrumental and instrumental-to-tree pairs. Correlations for the 11 high-elevation instrumental stations (circles) in 100-km distance classes, lagged 50 km, for JJA (solid) and A-S (dashed) average temperatures, and between tree-ring chronologies for ring width (triangles) and density (squares) and all instrumental stations in 50 km distance classes, lagged 25 km, are shown (A). For the instrumental-to-tree pairs, the exact period used depends individually on the end date of the tree-ring chronologies, but is computed within the 1933–1998 maximum period. For comparison, the tree-to-tree results from Fig. 3 and the tree-to-instrumental results are re-plotted in on the same axis in B.

(Frank and Esper, accepted). The common temperature signal across the network, and the relatively common signal within the tree sites related to this temperature signal, is captured by the common components of this network as demonstrated by PCA and the high spatial autocorrelation. The distances of significant (or positive) correlations for both the high-elevation seasonal temperature data and the tree-ring chronologies are substantially greater than the teleconnection threshold distances (where no correlation exists) as determined by Rolland (2002) in a more dense, but less spatially extensive study from the French Alps. On one hand the

east–west climatic gradient demonstrated with the PC analysis from the tree-ring chronologies in this study and the instrumental data in Böhm et al. (2001) indicate the potential for splitting into east and west temperature reconstructions. However, on the other side, the very high correlation along this east–west gradient likely lies well within the noise range of unexplained variance in tree-ring reconstructions, and the “costs” of having fewer tree-ring predictors in an area, do not seem to outweigh the benefits of splitting this data set into two or more east–west sub-regions. It is perhaps notable that these east–west climatic gradients seem to contrast with other sub-regional climatic splittings based on the north vs. south sides of the Alps (e.g., Pfister, 1999; Böhm et al., 2001).

Monthly and seasonal correlations for all of the species with climate tend to show a generally similar climatic response as evidenced by the positive loadings on the first PC for both ring width and density chronologies. In detail, however, differences for the ring width chronologies exist. ABAL has a more unique response than the other three species, and seemingly has a more complex response to warm season temperatures. At the same time, this species seems to carry more of an annual temperature signal than the other species. The comparisons of climate response versus elevation are similar to those determined by others (e.g., Kienast et al., 1987). However, the scatter and existence of some (highly) positively correlating sites from elevations well below the treeline suggest that a useful, positive, temperature response can be derived from some of these sites as well. Perhaps similarly, for example, Esper et al. (in review) found substantial common signals between trees growing near the upper-timberline with those from lower elevation sites, in a network of temperature sensitive juniper trees from Western Central Asia.

It is widely known that in comparison to ring width data, density data possess (i) a much greater common signal rather independent of species and site ecology, (ii) substantially higher correlations with climate data, and (iii) more year-to-year variation and fewer long term trends (e.g., Schweingruber et al., 1979; D’Arrigo et al., 1992; Wilson and Luckman, 2003). Our results support these “rules”. The comparison of the unfiltered and high- and low-pass filtered ring width and density responses to climate (Table 3) are an indication that the density data possess a greater fraction of their signal in the higher-frequency domains. This feature, however, possibly suggests limitations in the ability to retain lower-frequency variations (Briffa et al., 1998). Perhaps autocorrelation (and low-frequency variations) in the climate itself becomes more easily lost in the density parameter hidden by its exceptionally strong ability to pick up year-to-year fluctuations. However, conversely, the ring width parameters might possess more low-frequency variations than the climate itself, with their

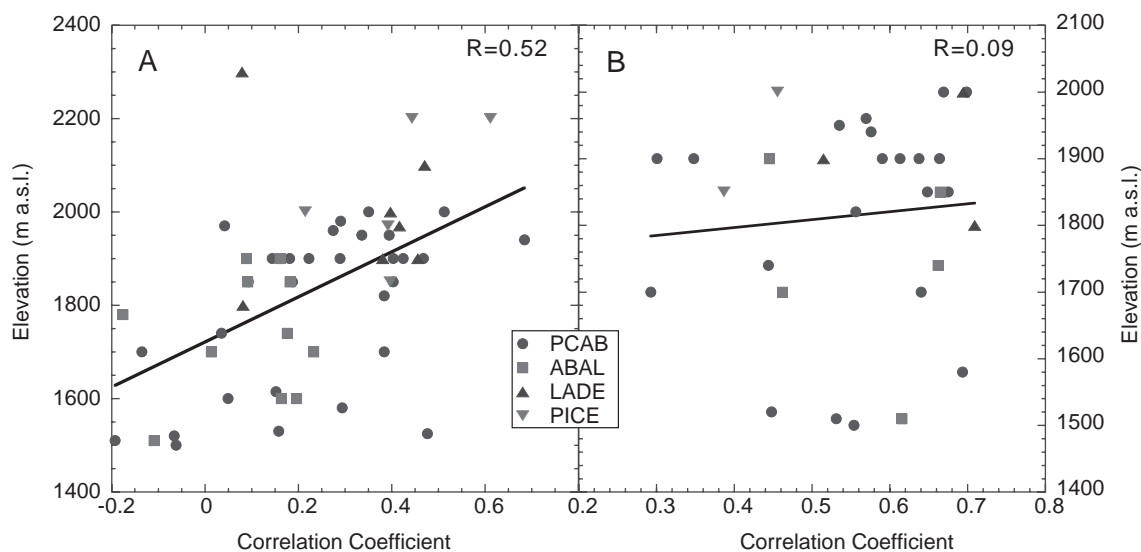


Fig. 8. Comparison of seasonal correlations as a function of elevation (A) for ring width and JJA temperature and (B) for density and A–S temperature. Linear fits are based on all data independent of species.

tendencies towards greater persistence and biological and environmental feedbacks. It is difficult to test the validity of these statements, however, as essentially all statistical tests are comparisons in the high-frequency domain (Esper et al., 2001).

The differences in representation of the four species included in this network may partially serve as an indicator for thoughts and findings of prior research on their climatic usefulness. It seems noteworthy that LADE and PICE are vastly underrepresented in the current network. The suitability of LADE for climatic reconstruction has been questioned (e.g., Schweingruber, 1985) because of the periodic population waves of the larch budmoth, and their feeding on LADE needles, which typically cause growth reductions in the year and generally subsequent years from the attack. While we have not conducted a detailed analysis of the larch wood or their chronologies, we have found some notable characteristics of this species. The LADE chronologies yielded some of the highest correlations with climate for both the ring width and density parameters. The high correlations between this species and the other chronologies also indicate its common signal due to climate. As this species is long-lived there is good potential for the development of climate-sensitive millennial-long chronologies utilizing living and historical material from buildings, for example (Büntgen et al., accepted).

Similarly, PICE and its suitability for climatic reconstructions has been questioned, along with other five needles pines (Schweingruber, 1985) primarily, for the density parameter. As has been previously noted (Schweingruber, 1985), we found limitations of this

species as well, with the correlations between maximum latewood density and climate for the PICE being consistently lower than those for the other three species. Nevertheless, ring width chronologies of PICE portray a somewhat different picture. Correlations with the monthly and seasonal meteorological data are among the highest with PICE ring width data. These chronologies also have the highest within and between species correlations. The low R_{bar} values of PICE, perhaps indicates that this species tends to be less sensitive to year-to-year climatic variations, and therefore seem to contain strengths in the multi-year to lower frequency time scales. For example, climatic modeling with the closely related *Pinus siberica* Du Tour in Mongolia yielded strongest relationships with temperatures averaged over 4 years (D'Arrigo et al., 2001).

As the LADE and PICE seem to have been somewhat neglected in terms of consideration for climatic reconstructions, we believe that these species have great potential in future studies. Overall, the quite significant common signals obtained over space (Central and Western Alps), between species, and within the tree-ring parameters (ring width and maximum density) demonstrates the potential to develop JJA and A–S temperature reconstructions using combined variance fractions from the whole network. However, from the comparisons shown here, it seems more important for the objective of temperature reconstructions to develop more long chronologies. Many of the chronologies in the network begin after 1700. The common signal across the network suggests that the specific location of potential future chronologies is not as important as their combined length.

Acknowledgements

We thank W. Elling, H. Fritts, W. Hüsken, F. Meyer, B. Neuwirth, R. Niederer, C. Rolland, F. Schweingruber, F. Serre, L. Tessier and K. Treydte for tree-ring data obtained directly or through the ITRDB and R. Böhm for meteorological data; and R. Wilson, F. Schweingruber, U. Büntgen and K. Treydte for comments and discussions; and P. Brown and an anonymous reviewer for additional comments and suggestions. Supported by the European Union Project ALP-IMP (BBW 01.0498-1) and the Swiss National Science Foundation (NCCR-VITA).

References

- Auer I, Böhm R, Maugeri M. A new long-term gridded precipitation data-set for the Alps and its application for map and alpcim. *Journal for Physics and Chemistry of the Earth* 2000;26(Part B):421–4.
- Baumann F, Kaiser KF. The Muletta debris fan, eastern Swiss Alps: a 500-year debris flow chronology. *Arctic, Antarctic, and Alpine Research* 1999;31:128–34.
- Böhm R, Auer I, Brunetti M, Maugeri M, Nanni T, Schöner W. Regional temperature variability in the European Alps 1760–1998 from homogenized instrumental time series. *International Journal of Climatology* 2001;21:1779–801.
- Briffa KR. Annual climate variability in the Holocene: interpreting the message of ancient trees. *Quaternary Science Reviews* 2000;19:87–105.
- Briffa KR, Jones PD, Schweingruber FH. Summer temperature patterns over Europe: a reconstruction from 1750 A.D. based on maximum latewood density indices of conifers. *Quaternary Research* 1988;30:36–52.
- Briffa KR, Schweingruber FH, Jones PD, Osborn TJ, Shiyatov SG, Vaganov EA. Reduced sensitivity of recent tree-growth to temperature at high northern latitudes. *Nature* 1998;391:678–82.
- Briffa KR, Osborn TJ, Schweingruber FH, Jones PD, Shiyatov SG, Vaganov EA. Tree-ring width and density data around the Northern Hemisphere, Part 1: local and regional climate signals. *The Holocene* 2002a;12:737–57.
- Briffa KR, Osborn TJ, Schweingruber FH, Jones PD, Shiyatov SG, Vaganov EA. Tree-ring width and density data around the Northern Hemisphere, Part 2: spatio-temporal variability and associated climate patterns. *The Holocene* 2002b;12:759–89.
- Brockmann-Jerosch H. Baumgrenze und Klimacharakter. Pflanzengeographische Kommission der Schweizerischen Naturforschenden Gesellschaft, Beiträge zur geobotanischen Landesaufnahme. Rascher: Zurich; 1919. p. 6.
- Büntgen U, Esper J, Frank DC, Nicolussi K, Schmidhalter M. A 1052-year alpine tree-ring proxy captures warmest summer temperatures in the last decade. *Climate Dynamics*, accepted.
- Cherubini P, Piussi P, Schweingruber FH. Spatiotemporal growth dynamics and disturbances in a subalpine spruce forest in the Alps: a dendroecological reconstruction. *Canadian Journal of Forest Research* 1996;26:991–1001.
- Cook ER. A time series analysis approach to tree-ring standardization. PhD dissertation, University of Arizona, Tucson AZ, 1985.
- Cook ER, Peters K. The smoothing spline: a new approach to standardizing forest interior tree-ring width series for dendroclimatic studies. *Tree-Ring Bulletin* 1981;41:45–53.
- Cook ER, Peters K. Calculating unbiased tree-ring indices for the study of climatic and environmental change. *The Holocene* 1997;7:361–70.
- Cook ER, Krusic PJ, Jones PD. Dendroclimatic signals in long tree-ring chronologies from the Himalayas of Nepal. *International Journal of Climatology* 2003;23:707–32.
- D'Arrigo RD, Jacoby GC, Free R. Tree ring width and maximum latewood density at the North American tree line: parameters of climatic change. *Canadian Journal of Forest Research* 1992;22:1290–6.
- D'Arrigo R, Jacoby G, Frank D, Pederson N, Cook E, Buckley B, Nachin B, Mijiddorj R, Dugarjav C. 1738 years of Mongolian temperature variability inferred from a tree-ring width chronology of Siberian pine. *Geophysical Research Letters* 2001;28:543–6.
- Dittmar C, Elling W. Jahrringbreite von Fichte und Buche in Abhängigkeit von Witterung und Höhenlage. *Forstwissenschaftliches Centralblatt* 1999;118:251–70.
- Esper J. Long term tree-ring variations in Junipers at the upper timberline in the Karakorum (Pakistan). *The Holocene* 2000;10:253–60.
- Esper J, Neuwirth B, Treydte K. A new parameter to evaluate temporal signal strength of tree ring chronologies. *Dendrochronologia* 2001;19:93–102.
- Esper J, Cook ER, Schweingruber FH. Low-frequency signals in long tree-ring chronologies for reconstructing of past temperature variability. *Science* 2002a;295:2250–3.
- Esper J, Schweingruber FH, Winiger M. 1300 years of climatic history for Western Central Asia inferred from tree-rings. *The Holocene* 2002b;12:267–77.
- Esper J, Shiyatov SG, Mazepa VS, Wilson RJS, Graybill DA, Funkhouser G. Temperature-sensitive Tien Shan tree ring chronologies show multi-centennial growth trends. *Climate Dynamics* 2003;8:699–706.
- Esper J, Frank DC, Treydte K, Büntgen U. On the palaeoclimatic relevance of 28 juniper tree sites in monsoonal to continental Western Central Asia. *Netherlands Journal of Geosciences*, in review.
- Frank DC, Esper J. Temperature reconstructions and comparisons with instrumental data from a tree-ring network for the European Alps. *International Journal of Climatology*, accepted.
- Fritts HC. *Tree rings and climate*. Academic Press: London; 1976.
- Gärtner H, Stoffel M, Lièvre I, Monbaron M. Tree ring analyses and detailed geomorphological mapping on a forested debris flow cone in Switzerland. In: Rickenmann D, Chen Ch, editors. *Debris flow hazards mitigation: mechanics, prediction, and assessment*, vol. 1, 2003. p. 207–17.
- Holmes RL. Computer-assisted quality control in tree-ring dating and measurement. *Tree-Ring Bulletin* 1983;43:69–78.

- Hüsken W, Schirmer W. Drei Jahrringchronologien aus den Prager Dolomiten/Südtirol. *Dendrochronologia* 1993;11:123–37.
- Jacoby GC, D'Arrigo R. Reconstructed northern hemisphere annual temperature since 1671 based on high-latitude tree-ring data from North America. *Climatic Change* 1989;14:39–59.
- Kienast F, Schweingruber FH, Bräker OL, Schär E. Tree-ring studies on conifers along ecological gradients and the potential of single-year analyses. *Canadian Journal of Forest Research* 1987;17:683–96.
- LaMarche VC, Fritts HC. Tree rings, glacial advance, and climate in the Alps. *Zeitschrift für Gletscherkunde und Glazialgeologie* 1971;7:125–31.
- Meyer FD, Bräker OU. Climate response in dominant and suppressed spruce trees, *Picea abies* (L.) Karst., on a subalpine and lower montane site in Switzerland. *Ecoscience* 2001;8:105–14.
- Motta R, Nola P. Dendrochronological signal in three stone pine (*Pinus cembra* L.) chronologies from the western Italian Alps. *Dendrochronologia* 1996;14:43–57.
- Neuwirth B, Esper J, Schweingruber FH, Winiger M. Site ecological differences to the climatic forcing of spruce pointer years from the Löttschental, Switzerland. *Dendrochronologia* 2004;21:69–78.
- Nicolussi K, Schiessling P. Establishing a multi-millennial *Pinus cembra* chronology from the central Eastern Alps. In: Kaennel DM, Bräker OU, editors. International conference of tree-rings and people. Davos, 22–26 September, 2001. p. 87.
- Osborn TJ, Briffa KR, Jones PD. Adjusting variance for sample-size in tree-ring chronologies and other regional-mean time-series. *Dendrochronologia* 1997;15:89–99.
- Paulsen J, Weber UM, Körner Ch. Tree growth near treeline: abrupt or gradual reduction with altitude? *Arctic, Antarctic, and Alpine Research* 2000;32:14–20.
- Pederson N, Jacoby GC, D'Arrigo RD, Cook ER, Buckley BM. Hydrometeorological reconstructions for northeastern Mongolia derived from tree rings: 1651–1995. *Journal of Climate* 2001;14:872–81.
- Petitcolas V, Rolland C. Dendroecological study of three subalpine conifers in the region of Briançon (French Alps). *Dendrochronologia* 1996;14:247–53.
- Pfister C. *Wetternachhersage: 500 Jahre Klimavariationen und Naturkatastrophen (1496–1995)*. Haupt: Bern; 1999.
- Richman MB. Rotation of principal components. *Journal of Climatology* 1986;6:293–335.
- Rigling A, Bräker O, Schneiter G, Schweingruber F. Intra-annual tree-ring parameters indicating differences in drought stress of *Pinus sylvestris* forests within the Ericopinion in the Valais (Switzerland). *Plant Ecology* 2002;163:105–21.
- Rolland C. Tree-ring and climate relationships for *Abies alba* in the internal Alps. *Tree-Ring Bulletin* 1993;53:1–11.
- Rolland C. Decreasing teleconnections with inter-site distance in monthly climatic data and tree-ring width networks in a mountainous Alpine Area. *Theoretical and Applied Climatology* 2002;71:63–75.
- Rolland C, Petitcolas V, Michalet R. Changes in radial tree growth for *Picea abies*, *Larix decidua*, *Pinus cembra* and *Pinus uncinata* near the alpine timberline since 1750. *Trees* 1998;13:40–53.
- Rolland C, Desplanque C, Michalet R, Schweingruber FH. Extreme tree rings in spruce (*Picea abies* [L.] Karst.) and fir (*Abies alba* Mill.) stands in relation to climate, site, and space in the Southern French and Italian Alps. *Arctic, Antarctic, and Alpine Research* 2000;32:1–13.
- Schweingruber FH. Dendroecological zones in the coniferous forests of Europe. *Dendrochronologia* 1985;3:67–75.
- Schweingruber FH. *Tree rings and environment: Dendroecology*. Haupt: Berne; 1996.
- Schweingruber FH, Briffa KR. Tree-ring density networks for climate reconstruction. In: Jones PD, Bradley RS, Jouzel J, editors. *Climatic variations and forcing mechanisms of the last 2000 years*. NATO ASI Series, vol. 141, 1996. p. 43–66.
- Schweingruber FH, Bräker OU, Schär E. Dendroclimatic studies on conifers from central Europe and Great Britain. *Boreas* 1979;8:427–52.
- Schweingruber FH, Bräker OU, Schär E. Temperature information from a European dendroclimatological sampling network. *Dendrochronologia* 1987;5:9–33.
- Schweingruber FH, Bartholin T, Schär E, Briffa KR. Radiodensitometric-dendroclimatological conifer chronologies from Lapland (Scandinavia) and the Alps (Switzerland). *Boreas* 1988;17:559–66.
- Serre-Bachet F, Martinelli N, Pignatelli O, Guiot J, Tessier L. Evolution des températures du Nord-Est De L'Italie depuis 1500 AD. reconstruction d'après les cernes des arbres. *Dendrochronologia* 1991;9:213–29.
- Tessier L. Contribution dendroclimatologique à la connaissance écologique du peuplement forestier des environs des chalets de l'Orgère (Parc nationale de la Vanoise). *Travaux Scientifiques du Parc national de la Vanoise* 1981;11:29–61.
- Treydte K, Schleser GH, Schweingruber FH, Winiger M. The climatic significance of delta-13C in subalpine spruces (Löttschental/Swiss Alps). A case study with respect to altitude, exposure and soil moisture. *Tellus* 2001;53B:593–614.
- Urbinati C, Carrer M, Sodiro S. Dendroclimatic response variability of *Pinus cembra* L. in upper timberline forests of Italian eastern Alps. *Dendrochronologia* 1997;15:101–17.
- Weber UM. Dendroecological reconstruction and interpretation of larch budmoth (*Zeiraphera diniana*) outbreaks in two central alpine valleys of Switzerland from 147–. *Trees* 1997;11:277–90.
- Wigley TML, Briffa KR, Jones PD. On the average of correlated time series, with applications in dendroclimatology and hydrometeorology. *Journal of Climate and Applied Meteorology* 1984;23:201–13.
- Wilson RJS, Luckman BH. Dendroclimatic reconstruction of maximum summer temperatures from upper tree-line sites in interior British Columbia. *The Holocene* 2003;13:853–63.
- Wilson RJS, Topham J. Violins and climate. *Theoretical and Applied Climatology* 2004;77:9–24.